UNIVERSITY OF WEST BOHEMIA

Applied and Computational Mechanics 4 (2010) 57–66

Applied and Computational Mechanics

A Comparison of Flow Field Characteristics from PIV Experiment Measurement to Numerical Simulation behind a Spacer in a Vertical Pipe

D. Lávička[a,*]

[a] *Faculty of Mechanical Engineering, Department of Power System Engineering, University of West Bohemia, Univerzitní 22, 306 14 Plzeň, Czech Republic*

Received 31 August 2009; received in revised form 19 July 2010

Abstract

This paper describes the topic of measurement using a modern laser method (PIV) in an annular channel of very small dimensions. The annular channel simulates the flow area around a model of a fuel rod in the VVER nuclear reactor. The annular channel holds spacers which create obstacles to fluid flow. The spacers serve a number of important purposes. In the real nuclear reactor, the spacer holds a fuel rod in the fuel rod bundle. Another important function of the spacer is to influence the flow field characteristics, especially turbulence size, by the shape of the spacer. The value of the turbulence regulates the intensity of heat transfer between the fuel rod and the fluid. Therefore, it is very important to provide a correct description and analysis of the flow field behind the obstacle the spacer generates. The paper further looks into the solution of the same task using numerical simulation. The solution of this task consisted of setting the suitable boundary conditions and of setting the turbulence model for the numerical simulation. The result is a comparison of the flow field characteristics from the experimental measurement and the findings of the numerical simulation. The numerical simulation was carried out using commercial CFD software package, FLUENT.

Keywords: laser anenometry, PIV, numerical simulation, FLUENT, spacer, vertical annular tube

1. Introduction

The two-phase flow is a special type of flow where the running medium includes two components with different material and physical properties. This is, for example, flow of a liquid or gas containing solid particles, or flow of a mixture of liquid and gas media, that is, gas bubbles in a liquid. The two-phase flow is very common in industry and it plays a major role in delivering high efficiency in many technology processes, for example flow and transfer of heat in energy and chemical industry, etc. However, certain physical processes that occur during the flow have not been understood and described in full. Bearing these facts and current needs in mind, the FST KKE laboratory has built a special experimental apparatus to address the topic of heat transfer in nuclear reactor fuel rods. Research activities have been started at this apparatus during this year. The main topic is generation of gas bubbles that affect flow and heat transfer from the heated wall into ambient environment. The ability to predict the size, development and movement of the steam phase, as well as other parameters that describe two-phase flow during the boiling process is paramount especially in the realm of nuclear reactor safety and in other industrial applications. In the domain of PWR and BWR nuclear reactors, this process

*Corresponding author. Tel.: +420 377 634 712, e-mail: dlavicka@ntc.zcu.cz.

is sometimes referred to as "boiling crisis". Two-phase turbulent flow in the boiling process contains a large number of bubbles, and together with heat transfer, it represents a highly complicated process. Upcoming years of research show direction towards a detailed description of the process, and to the definition of the boundary conditions for numerical simulations.

This paper focuses on the description of the preliminary research tasks which used the experimental and computational methods to analyze the flow field in the annular channel area at the model of the environment of a fuel rod. The analyses have so far been made for single-phase flow, that is, in cold equipment without heat transfer, and have been focusing at the turbulence area behind the spacer. The asset of these tasks is especially the comparison of the findings of experimental measurements to the numerical simulations. The experimental measurement used the modern laser method, PIV, at the annular channel area of very small dimensions, under normal water temperature. The numerical simulations were carried out using the FLUENT software package.

2. Experimental investigations

2.1. Experimental apparatus

The experimental apparatus (see Fig. 1) consists of a water circuit and a fuel rod model. The basic element of the water circuit is a dosing pump which allows setting the mass flow rate as required. Distilled or tap water is used as the coolant; it is taken from a reservoir with a capacity of ca. 200 L. In order to harmonize flow, a pulse damper is located behind the pump. The main parts of the experimental apparatus are the input and output heads, connected with a glass pipe which enables observation of the processes described above. A stainless-steel pipe with spacers is located within the glass pipe.

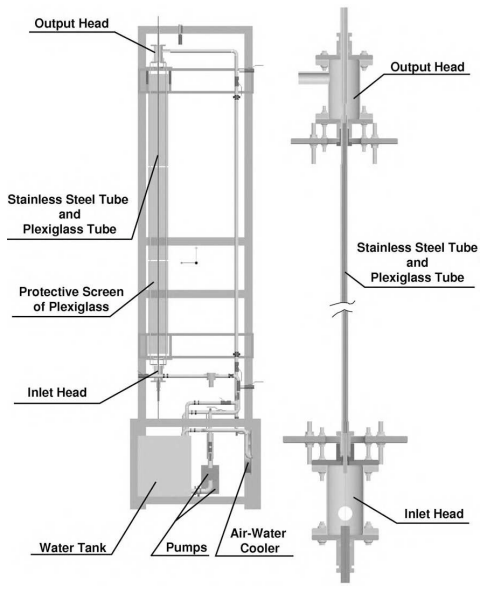

Fig. 1. Experimental apparatus

The spacers installed at the heated pipe play several important roles. Firstly, they provide alignment within the glass pipe shown in Fig. 2. The spacer also acts as vortex generator. This is where the liquid is forced to flow around the spacer and flow turbulence occurs behind the spacer. The size and intensity of the vortex area directly affects heat transfer between the heated stainless-steel pipe and the flowing coolant in the annular area. The investigated area is described in Fig. 2.

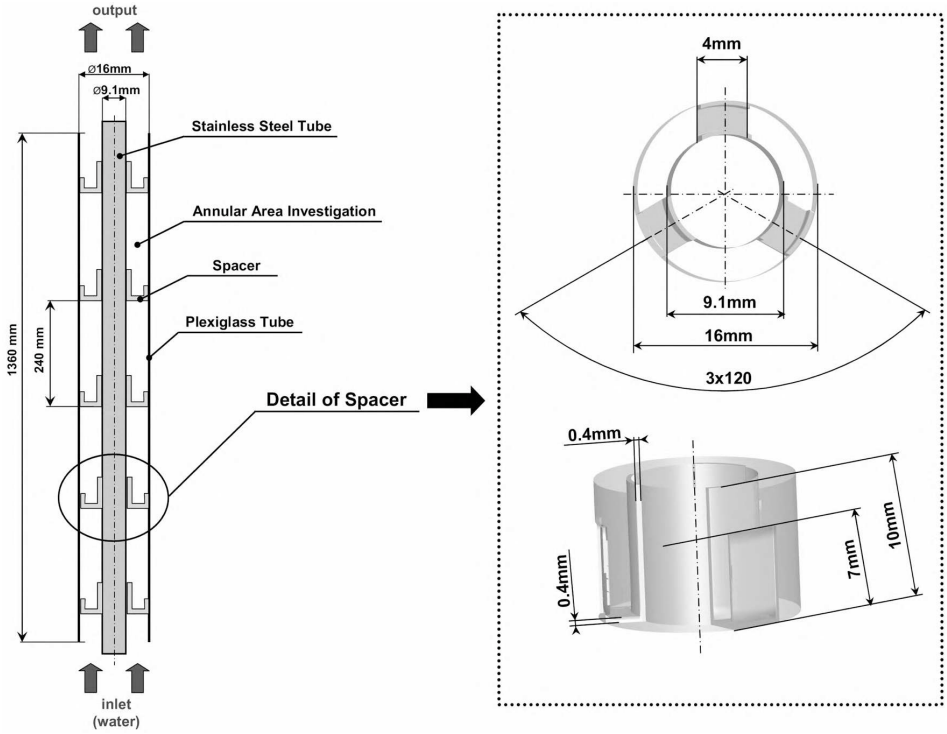

Fig. 2. Fuel rod model with a detailed view of the spacer

Until now, only one spacer type has been used for the measurement. This spacer type has been designed especially for correct alignment of the heated rod inside the glass pipe. The shape of the spacer was designed in consideration of the ease of preparation and manufacture thereof. A detailed view of the spaces is shown in Fig. 2. The spacer is U-shaped; the length of its sides is asymmetrical. The longer side is welded to the heated rod. The shorter side flexibly lean on the glass pipe and the spacer flexible holds stainless steel inside the glass pipes. The size of spacer is described in Fig. 2. The model of a fuel rod contains about five linear array of spacer and line spacing is 240 mm to overall length 1 405 mm. The blockage ratio of the spacer is 0.7. This value was calculation as ratio between the spacer surface and the annular flow section area. In the future, measurement of spacers at fuel rods in a VVER 1000 nuclear reactor will be taken. This spacer type derives from the original project proposal type for tests regarding the “heat transfer crisis”. The information about and the properties of current spacers will be applied in the design solution of proprietary spacers.

2.2. Measurement using PIV (Particle Image Velocimetry)

The applied measurement method, PIV (see Fig. 3), is based on monitoring particle movement in a defined volume of liquid. The principle of velocity measurement is based on the premise of equal rate of velocity in both the particles and the liquid, when the travel of a group of particles is measured within given time. Assessment of the measured travel uses a number of methods which depend on the technology of measurement technique and data recording; in most cases, this is cross or adaptive correlation. An example process from the actual measurement until the assessment of the received images is shown in Fig. 3.

The used method, PIV, at the portrayed model of a fuel rod in Fig. 2 shows the relevant dimensions of both the investigated flow channel and the spacer. Fig. 2 indicates that the dimensions of the monitored area are very small. The maximum channel width is 3.5 mm; the size of the monitored area is defined by the camera used for capturing the image. These small dimensions are on the edge between "normal"-PIV and "micro"-PIV (μ-PIV). This measurement was very sensitive as to the accuracy of the settings of the laser beam and the recording camera. The accuracy of the measurement also depended on the size of the particles used, velocity gradient, interval length between two flashes, laser beam intensity, etc.

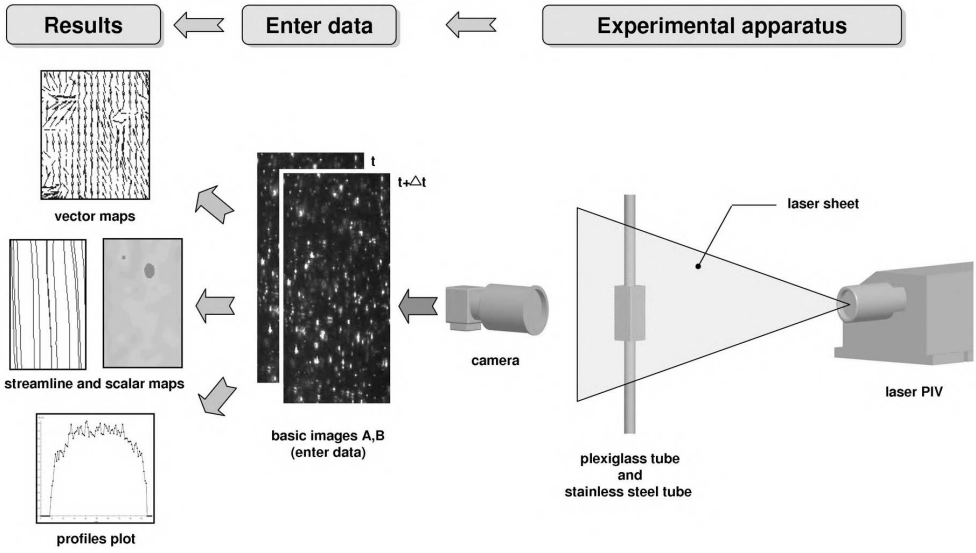

Fig. 3. Diagram and principle of experiment measurement using the PIV method

The refractive index is next very important accuracy factor in measuring for interface between air-plexiglass and water-plexiglass. Water has a refractive index close to 1.33, air 1.000 3 and plexiglass 1.488. Index of refractive values can be influence an effect on obtained images from PIV and results of fine measuring. This previous describing factors were solved during design plexiglass tube and final shape and construction eliminate this problems. Design of plexiglass tube is shown to figure 3 and 4. Greatest requirements were for interface between air-plexiglass, because this interface causes bigger problems with accuracy. Solutions are flat surface for incidence of laser beam and reading of images, which it's created by the transition element on the plexiglass tube. This transition element is block with through hole in center.

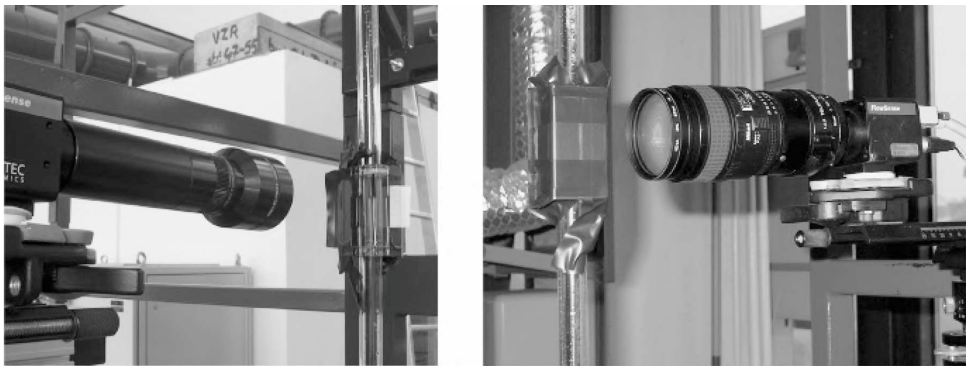

Fig. 4. Used cameras for record and laser beam on area investigation

Second interface between water-plexiglass is not more important, because values of index reflective are similar.

The measurement was not only sensitive as to the operational setting of the equipment, but also in terms of human interaction around the experiment. Even the slightest of movement around the experimental apparatus caused vibration which would result in depreciation of the acquired images.

The experiment was carried out using a borrowed telecentric lens Navitar ELWD Macro Invarotar by Melles Griot (see Fig. 4 left). The telecentric lens was used to monitor an area of ca. 70×70 mm from a distance of 120 mm. The effective distance was defined by the focal length of the lens. A minor disadvantage of the lens was the square field of view; yet the corners of this field are not visible. That is why only a fraction of the recorded field of view is used for assessment. This fact reduced the final image to an area of ca. 5×5 mm.

During the experiment, other alternatives were tested, such as using a Nikon AF Micro Nikkor 60 f/2.8D lens upgraded with secondary lens and teleconverters (see Fig. 4 right). A combination of several secondary lens and teleconverters returned similar image size as in the case with the telecentric lens. This solution with a Nikon AF Micro Nikkor 60 f/2.8D was not feasible, as the lens was heavy, large in size, and extremely sensitive to vibration from the experimental apparatus. The results taken by this lens arrangement have also been kept; a comparison between the methods used in image acquisition is being prepared. The resulting image was 9×9 mm in size, from an effective distance of 170 mm.

Both lens were attached to a Flow Sense 4M 1/2" CCD chip purchased from the Dantec company which was used to capture the images from the lens. The laser beam was excited by NewWave Research Model 25 300Solo 200XT-15 Hz, also manufactured by Dantec. Laser beam intensity was set according to the aperture numbers of the respective lens. Data recording and processing was carried out in the software supplied to the PIV equipment, Dynamic Studio v. 2.30, on PC Dell Precision PWS 690 and 390 workstations, on the Windows XP Professional platform. For processing the velocity field and profile, all instances used 300 pairs of images. Adaptive correlation of these images returned detailed description of the flow field with the actual state of the velocity field. The supplied software was used to calculate the average of these 300 assessed velocity fields to return the average flow field over time, similarly to the numerical simulation.

3. Numerical simulation

Numerical simulation was used for solving the same spacer as at the experimental apparatus within a plexiglass tube. The spacer is used to secure the centered position of a stainless-steel pipe that runs along the center axis of the plexiglass tube. A brief description of the flow channel around the stainless-steel pipe is shown in Fig. 2. This paper will only look into the flow around the stainless-steel rod with spacers. Numerical simulation will also run at the constant air temperature equal to the experiment in the laboratory. The findings focus on the velocity and pressure parameters within the annular flow channel. In the future, these numerical simulations will include heating of the stainless-steel rod, as well as the study of heat transfer into the ambient environment and into the steel rod.

3.1. Geometry and mesh

The computational geometry and mesh were created in the Gambit software package. The base of the numerical model is an area in the shape of the spacer, projected perpendicularly onto a plane. In this plane, the Gambit software used quad elements to create the surface mesh. The number of surface elements in the plane is approximately 25 000 cells. Fig. 5 shows an example of the surface mesh around Spacer 3.

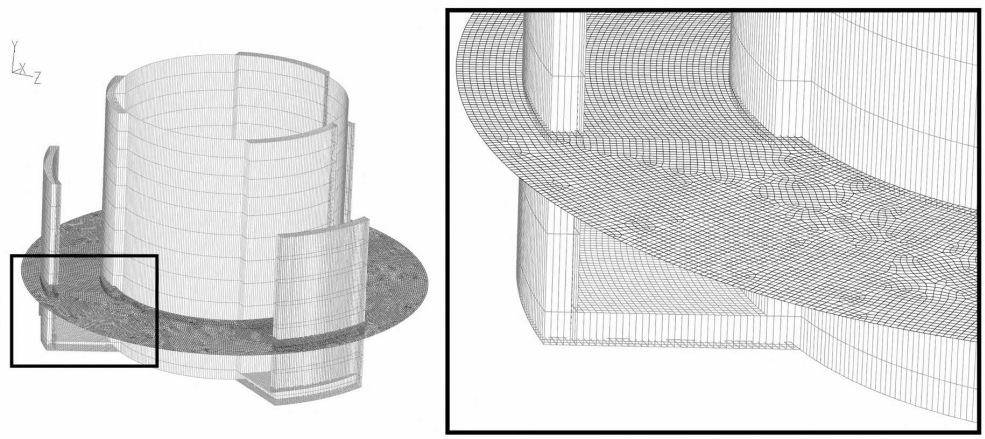

Fig. 5. Detailed view of surface mesh around spacer

This basic plane with surface elements is extending along the "y" axis at a total length of 1 360 mm by the function "Cooper Mesh Scheme Type" (similar function is sweep). This function observes equal distribution surface cells between two planes and volume cell is created third co-ordinate axis.

Element height (i.e. length along the "y" axis) is built at floating distances between individual nodes. Details are added to element height only around the individual spacers. This area generates large vortex of the flow; therefore, the fineness (element size in height) of the mesh affects the accuracy of numerical simulation findings. The height of the spacer was defined as 10 cells within a distance of 10 mm, and for the area between the spacers 80 cells were defined within a distance of 230 mm. The total element count throughout the height of the model was 495, and the total count of cells used at the volume mesh of the annular channel with spacers was approximately 12.5 million. The basic layout and dimensions are shown in Fig. 2. The

stainless-steel pipe in the center of the model holds a total of 5 spacers with distance of 240 mm between the individual spacers.

The boundary conditions for numerical simulation are shown in Fig. 2; these conditions are based on the experimental apparatus as per Fig. 1. The lower part of the flow channel holds a defined limiting input condition of "mass-flow inlet" to specify the flow rate of water. The flow rate was set at 0.34 kg/sec, which represents a flow rate of approximately 20 liters per minute. The upper side of the computational geometry had a defined output boundary condition of "pressure-outlet".

3.2. Numerical model

The numerical simulation was divided into a series of several steps to improve the stability and, above all, the accuracy of the calculation. The calculation of the flow field in the annular flow channel around the spacer was concluded using the FLUENT 6.3.26 CFD software package. The flow media was tap water, same as in the experiment. The mathematical description of the flow is given by the set of Navier-Stokes equations for turbulent viscous isothermal flow. The calculation was commenced in the stationary mode, with a pressure-based solver with the *realizable k-*ε turbulence model in the 1st precision order with 4 000 iterations. As the next step, the calculation was set to non-stationary mode in 2nd precision order with the *Large Eddy Simulation (LES)* and sub-grid eddy viscosity model is Dynamic Kinetic Energy Transport. For the first 200 time steps was set 60 iterations in one time step and length of time step was choose 0.000 5 seconds.

The result showed good convergence of under-relaxation factors; that is why the number of iterations was reduced to 40 in the remaining time steps. In the end, 800 time steps in the non-stationary mode were calculated in order to receive a converged flow field in the annular cross-section behind the spacer in the vertical tube. The next part of the calculation had 700 more time steps as a non-stationary calculation with average values. These calculated results of average flow field were used for comparison with the results received through PIV.

4. Results

Fig. 6 shows the development of the flow field in the individual planes in the area around Spacer No. 3 at velocity v_y (y – *component of velocity* v). A total of 9 cross-sections were made through the annular flow channel within 700 mm and 800 mm. The exact positions of the individual cross-section planes are shown in Fig. 6. The sections on the left show instantaneous velocity v_y in Time Step 1 500. The instantaneous velocities v_y can be compared to velocity v_y^*, which was calculated as a mean value (average) in time t after 700 time steps (on the right side). This results shows cross-sectional planes with the sampling data from time statistic (weighted average) velocity of v_y^*.

The instantaneous velocities in these planes show a highly non-stationary flow field for velocity v_y in time t. Another item worth mentioning is the asymmetrical distribution in each of the three sections which are the result of dividing the flow channel by spacers. These results in the individual planes across the vertical flow field behind the spacer indicate that the simulation of the flow channel with a periodic boundary condition is slightly complicated.

The largest differences in actual velocity are found in the planes positioned from 710 mm to 730 mm (region of spacer).

The next Fig. 7 shows the positions of the planes in the annular flow channel where the profiles of velocities v_y and v_y^* were read. The positions for reading the velocity profiles are

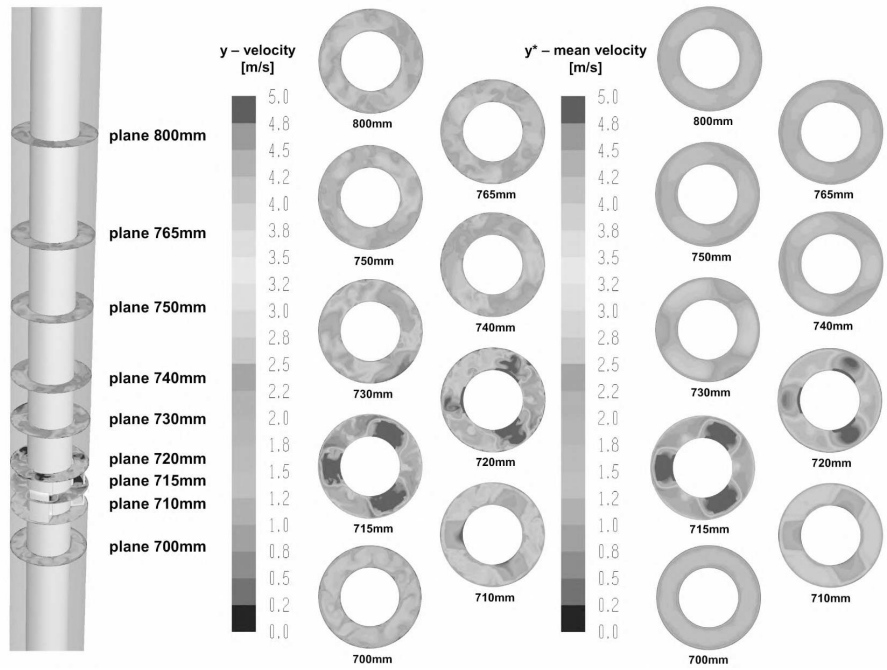

Fig. 6. Development flow field of v_y and v_y^* in planes around Spacer No. 3

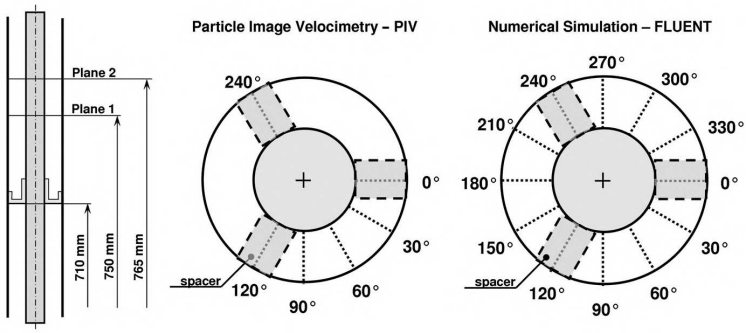

Fig. 7. Reading planes and angles for comparison of velocity profiles

given by the angle they are positioned in in respect of the spacer. The velocity profiles were read in two planes, 750 mm and 765 mm.

Thus defined planes were identical for the numerical simulation and for the experimental measurement using the PIV. In the case of numerical simulation, the velocity profiles were read at 30° increments throughout the circumference of the annular flow channel around the fuel rod. In numerical simulation, comparisons may be taken also in the flow fields of the individual sections defined by the spacers. At the experimental measurement PIV, the velocity profiles were also read at 30° increments, but only from one section of the flow channel. In the case of further experimental measurement, a comparison of the velocity profile between individual

sections would be feasible. The situation and marking of the individual velocity profiles are shown in Fig. 7.

Fig. 8 provides the important juxtaposition of the results using both methods: the PIV experimental measurement and the FLUENT numerical simulation. Velocity fields are compared for average values or data sampling from time statistic. These problems of comparing results are describing previous chapters. The velocity profiles are compared in planes 750 mm and 765 mm. The first plane, 750 mm, was used for comparison of the angles of $0°, 30°, 60°, 90°$, whereas the other plane, 765 mm, was used for the angles of $0°$ and $60°$. The best correspondence between the experimental measurement and the numerical is seen at the velocity profile at 750mm and the angle of $30°$. On the other hand, the worst correspondence is indicated at the plane of 750 mm and the angle of $0°$, where the velocity field was measured immediately above the spacer. The results of the numerical simulation exhibit higher velocity v_y^* than in the experimental measurement. This measurement is likely to be affected by the wake behind the spacer, an area where the flow field is highly non-stationary and major velocity fluctuations occur. Looking at the plane 15 mm higher, i.e. 765 mm, the velocity profile shows very good concordance between the experimental measurement and the numerical simulation. The results for these two planes at the angle of $0°$ indicate that the 750mm plane is located in the wake or on its boundaries. However, Plane 765 mm is probably located outside the wake of the spacer. All other measured and shown profiles show very good concordance between the experimental measurement PIV and the CFD numerical simulation.

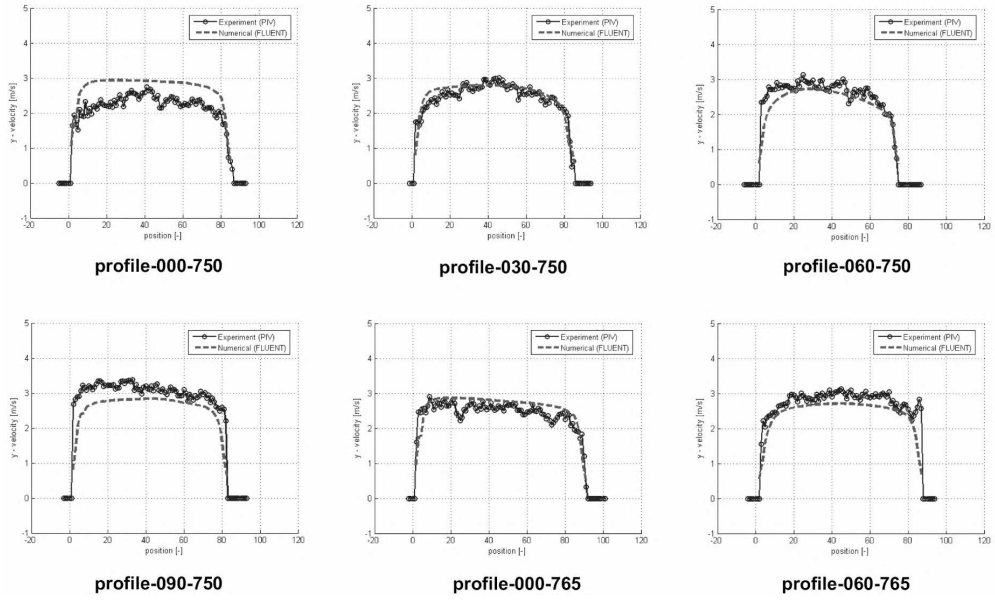

Fig. 8. Comparison of velocity profiles between the numerical simulation and results from PIV

5. Conclusion

The aim of this paper was the measurement and mapping of flow field behind the obstacle of spacers located in the annular channel of a model of a VVER nuclear reactor fuel rod. The

description of the flow field was received by experimental measurement using the PIV method in the annular flow channel of very small dimensions. The presented results of the experimental measurement are complemented with a comparison with the results of numerical simulation. The difficulty of the numerical simulation lies in the choice of the vortex model and the fineness of the numerical model mesh which affects the time and hardware constraints of the calculations. On the other hand, the experimental measurement required the solution of optical issues (reflections, laser pass-through and capturing the image of the circular plane, etc.) related to the annular channel of very small dimensions. In spite of the issues stated above, the results indicate very good concordance between the experimental measurement and numerical simulation.

The description of the flow field will be used for analysis of the flow profile of a liquid in the annular flow channel in various configurations and shapes of spacers. The spacer shape and configuration has a major impact on flow vortex properties which, in turn, affect heat transfer from the stainless-steel pipe (fuel rod) into the environment. The data received will be later used especially in numerical simulation of multi-phase flow with heat transfer from the steel pipe into the environment. The results of numerical simulation will be continuously validated by state-of-the-art experimental methods at the experimental apparatus for the sake of studies in multi-phase flow with heat transfer.

Acknowledgements

This work was supported by the Czech Grant Agency project No. 101/09/P056. We would also like to thank the MetaCentrum project for their Linux PC cluster computational support.

Last but not least, I would like to express my gratitude to Yanick Knapp, a specialist in laser anenometry from Avignon University, France, who assisted us in setting the equipment and in the first measurement stage and contributed in building our experience in this aspect of experimental measurement.

I would like to use this opportunity to thank ing. Jan Novotný from the Fluid Mechanics and Thermomechanics Department at the ČVUT Prague.

References

[1] Lavicka, D.: Popis reseni numerickych simulaci v mezikruhovem prutocnem kanale okolo nerezove trubky. Stretnutie katedier mechaniky tekutin a termomechaniky, Jasna, Demanovska dolina, Slovensko, 2009. ISSN 1335-2938.

[2] Fluent 6 “User´s Guide”, 2007.

[3] Raffel, M., Willert, C., Wereley, S., Kompenhans j.: Particle Image Velocimetry: A Practical Guide. Second Edition, Springer, Germany, 2007. ISBN 978-3-540-72307-3.

[4] Tu, J. Y., Yeoh, G. H.: Development of a numerical model for subcooled bowling flow. 3rd International Conference on CFD in the Mineral and Process Industries. Melbourne, Australia, 2003.

[5] Hassan, Y. A.: Dancing Bubbles in Turbulent Flows: PIV Measurements and Analysis.

[6] Okawa, T, Ishida, T., Kataoka, I., Mori, M.: An experimental study on bubble rise path after the departure from a nucleation site in vertical upflow boiling. Experimental Thermal and Fluid Science 29, vol. 287–294, 2005.